Velocity dependence of the *K* Auger deexcitation of O^{7+} projectiles impinging on solid Cu(111) at 51 and 102 keV

A. Saal,* L. Aberle, R. Page,* J. Thomaschewski, and J. Bleck-Neuhaus
Department of Physics, University of Bremen, P.O. Box 330440, D-28334 Bremen, Germany

M. Grether and A. Spieler
Hahn-Meitner-Institute GmbH, 14109 Berlin, Germany

(Received 19 June 1996)

The time evolution of deexcitation of O^{7+} ions penetrating the (111) surface of Cu is studied by means of secondary electron spectroscopy. It is found that the filling of the *K* shell proceeds faster at 102 keV than at 51-keV ion energy, by about 10%. This velocity dependence is determined from a comparison of emission depth profiles, assuming straight-line trajectories for the ions. No further model is needed for the ion deexcitation or the solid-state interactions of the emerging Auger electrons. The model independence is based on three steps: (i) the emission depth profiles for different ion energies and angles are evaluated only in conditions where they are practically equal; (ii) the full *K* Auger electron spectra with their inelastic parts are obtained using matching pairs of measurements with O^{6+} projectiles; and (iii) the observation angles are adjusted to equalize, for both ion energies, the laboratory energies of the Auger electrons at emission as well as their solid-state interactions on their way to the surface. The present method can provide benchmark values for multistep cascade models of highly charged ion deexcitation in solids. [S1050-2947(97)04902-0]

PACS number(s): 34.50.Dy, 79.20.Rf

I. INTRODUCTION

The neutralization and deexcitation of highly charged ions while they are approaching and eventually penetrating a metal surface is a complex process of charge transfer and energy release [1–15]. During this relaxation process, the projectile ion performs a multistep cascade of electron transfer processes and deexcitation transitions which has attracted much interest in the last years. Measurements of the secondary electrons emitted during this process have provided information on the very short time scales involved. In these experiments, the clock to measure the time evolution of electron emission is given by the ion motion itself, since the incidence angle and energy determine an effective time window of observation which is opened when the ion enters the interaction zone with the surface, and is gradually closed as the ion reaches a depth from where the electrons can no more be detected [7,15].

Particular emphasis has been devoted to study the Auger electrons emitted during the filling of the deeply lying *K* shell hole in hydrogenlike projectiles of first row elements, $N^{6+} \ldots Ne^{9+}$. The final filling step occurs mainly through an atomiclike *KLL* Auger transition. This transition process itself is nearly independent of the interaction of the projectile with the solid, in contrast to the foregoing electron feeding to the *L* shell. During the motion through the solid, the projectile acquires *L*-shell electrons not only through Auger transitions from higher shells but also through a direct transfer from target states. This side feeding [2] process plays an important role in the acceleration of the *K* Auger emission, but is difficult to observe directly. It was first inferred qualitatively from the lack of projectile *L* Auger electrons observed in these reactions [2]. In subsequent studies, the development of the *K* Auger activity was inferred from the amount of electron-solid interaction seen in the spectra of the emerging K Auger electrons [4–7,10–14]. In this way, absolute estimates of the *L*-shell filling rates were derived, and the expected increase of side feeding with increasing ion velocity was found [11–14]. It is common to these important results that they were deduced from the experiments in a way which depends on two models, one for the ion transport within the solid, and the other for the electron transport toward the surface. The models available, however, are still quite approximative. They might appear either as strongly simplified [4–7,10–12], or as very detailed and involving a lot of parameters [13,14,16].

We report on an experiment aimed at examining the velocity dependence of the side feeding in a more direct way. In particular, we avoid the use of any model for the electron transport in the solid. Nevertheless, the depth distribution of emission will be evaluated by means of information contained in the complete spectrum of the emerging Auger electrons, particularly in the shape of the Auger peak in relation to its inelastic tail. The basic idea is to perform a comparative measurement of two spectra in such a way that, ideally speaking, a difference observed between them would already tell us that the underlying depth distributions of emission are different, too. In order to measure such a pair of *corresponding* spectra, all other possible reasons for different spectral shape and intensity must be eliminated.

Our method of how to achieve this in a practical sense is presented in Secs. II A and II B. In the real experiment (Sec. II C), we measure several pairs of corresponding spectra at different ion energies and angles of incidence until the con-

*Present address: Departamento de Física, Pabellón 1, Ciudad Universitaria, Facultad de Ciencias Exactas y Naturales, Universidad de Buenos Aires, 1428 Buenos Aires, Argentina.

ditions are found for which both spectra show the best agreement (Sec. III). This pair of energies and angles of incidence is then analyzed further, relying only on the fact that the underlying depth distributions of the Auger emission are practically equal. In this way the dependence of the deexcitation cascade on the ion velocity is tested, and is determined quantitatively in relative terms (Sec. IV A), without incurring the problems associated with a quantitative evaluation of the shape and intensity of the electron spectra themselves. This experimental result is then compared to predictions of existing cascade models, eventually after making a rough extrapolation to the ion energies used here (Sec. IV B).

The step of major importance in the experimental procedure is to extract from each total spectrum the contribution originated by the K Auger electrons alone. Hence the background caused by other mechanisms of electron excitation, mainly kinetic emission, must be removed not only under the Auger peak but also under its inelastic tail. Since different methods of background subtraction are in use in studies of the highly-charged-ion surface interaction [2,5,17], a particular effort was made in the present work to determine the spectral background (Sec. II B).

II. EXPERIMENT

A. Method of corresponding spectra

In the following we denote by $A_V(t)$ (activity function) the unknown time evolution of the KLL Auger emission for ions of velocity V, and by $S(E)$ the observed energy spectrum of the K Auger electrons after leaving the solid in the direction of detection. The link between the two functions is provided by the depth distribution of the emission sites of the K Auger electrons, $Q(z)$. The depth distribution $Q(z)$ depends strongly on $A_V(t)$, and it has an important influence on the shape and intensity, $S(E)$. These relations, in fact, allow us to study the activity function by means of measuring electron spectra. In general, however, they are too complex to permit a quantitative analysis of the spectrum without relying strongly on approximate models for the transport of the highly charged ions and of the emitted electrons through the solid [16,13,14]. Here we make an attempt to exploit these relations under the condition that the model dependence be eliminated as far as possible.

We first consider how the activity function determines the depth distribution of the emission. This relation becomes simple and practically model independent (even considering the yet poor knowledge of the exact scattering potential [18]) if the ions during the time interval of interest are moving at constant velocity along straight-line trajectories. Then all the ions reach a depth z at the same time t after surface impact. This time can be expressed as $t=z/V_n$, with $V_n=V\sin\Psi$ being the normal component of the ion velocity V, and Ψ the glancing angle of incidence. Hence, the depth distribution $Q(z)$ follows directly the time evolution of the K Auger emission: $Q(z)=A_V(z/V_n)/V_n$.

In practice, this greatly simplifying condition can be met, with sufficient accuracy, using ion beams of typically a few keV/amu and at not too small a normal velocity V_n. For the present experiment O^{7+} ions of energies $E_{\mathrm{ion1}}=102$ keV and $E_{\mathrm{ion2}}=51$ keV ($V_1=0.5$ a.u., $V_2=0.35$ a.u.) were directed against a Cu target at angles $\Psi\geqslant 20°$. Simulations made with the MARLOWE [19] and IOR [13] codes using different ion-ion scattering potentials (including, e.g., after Ref. [18]) confirmed the condition of straight-line trajectories.

The 102-keV ions were used at an incidence angle $\Psi_1=20°$ to define a reference emission profile held constant for all measurements. Different incidence angles were tried for the slower ions in order to find out at which angle Ψ_2 they would produce the same depth distribution.

The first trial value is $\Psi_2=29°$, where the ions of both energies have equal normal velocity $V_n=0.17$ a.u. If the time evolution of K Auger emission were independent of the ion velocity [*''intrinsic hypothesis,''* $A_{V_1}(t)=A_{V_2}(t)$], both depth distributions would be equal for this choice of Ψ_2. From the general picture of the deexcitation cascade it is expected, however, that the activity of slower moving projectiles develops slower [11,12]. The slower ions will produce the same depth distribution of emission as the faster ones, only at reduced normal velocity. This means reducing the angle of incidence to $\Psi_2<29°$. A reasonable lower limit for Ψ_2 is found, considering a case where the development of $A_V(t)$ would proceed at a speed which is proportional to the ion velocity. This hypothetical case would be true, e.g., if the KLL activity level were completely driven by collisions with the target atoms or electrons, but with no extra energy dependence. Under this *''collisional hypothesis''* the same level of activity would be reached after the same path length in the solid, independent of the ion velocity. The two ion beams would have different activity functions, $A_{V_1}(t)\neq A_{V_2}(t)$, but again the same emission depth distribution $Q(z)$ if $\Psi_2=\Psi_1$.

In reality, however, both the intrinsic and collisional contributions will be present in the emission time evolution. A collisional part of the whole process may be seen in the filling of the L shell, which is efficiently dominated by the side feeding, at the ion energies chosen here. This time constant will be as low as about a few a.u., as can be extrapolated from the results quoted above for other projectile-target combinations [10–14]. An intrinsic part of the deexcitation cascade may be expected for the time after the L shell has been filled. This part corresponds to the K Auger decay which has a time constant at least one order of magnitude longer than the L-shell filling [20]. It is seen that the major part of the time evolution is of intrinsic nature. The slower ions will need only slightly more time than the faster ones to emit their KLL Auger electron. Therefore, the best overall agreement of the depth distributions of emission can be expected for a Ψ_2 only a little bit less than the value 29° corresponding to equal vertical velocity.

Now we consider how a variation of the depth distribution can be inferred most directly and in the least model dependent way from observed differences between two electron spectra. This means minimizing all other effects that can produce a difference in the electron spectrum. In first place, an increasing depth of emission causes the Auger peak to decrease, and its inelastic tail to grow. Since similar variations can be produced, observing the electrons in a direction closer to the surface [16,21,22], a pair of spectra suited for this comparison must be detected at the same observation angle α with respect to the surface. Furthermore, the Auger peaks must have equal laboratory energy. A pair of electron

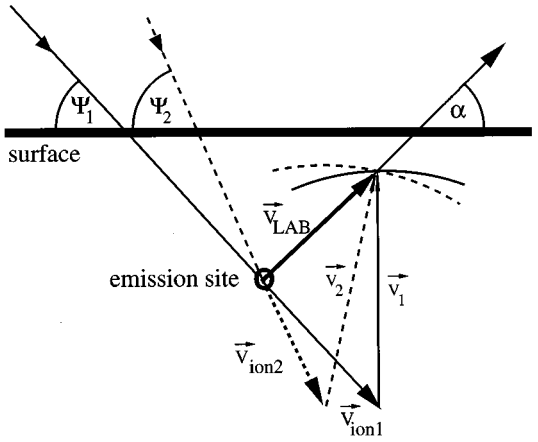

FIG. 1. Geometry for the method of corresponding spectra. The two ion beams have different velocities $\vec{V}_{\text{ion1}}$ and $\vec{V}_{\text{ion2}}$, but their Auger electrons have the same laboratory energy at the same angle of emergence from the surface, i.e., the same velocity vector $\vec{v}_{\text{LAB}}$ in the laboratory system. The end point of $\vec{v}_{\text{LAB}}=\vec{V}_{\text{ion1}}+\vec{v}_1=\vec{V}_{\text{ion2}}+\vec{v}_2$ is found as the intersection of the two circles drawn around the end points of the velocity vectors $\vec{V}_{\text{ion1}}$ and $\vec{V}_{\text{ion2}}$, with radius $|\vec{v}_1|=|\vec{v}_2|$ equal to the velocity of the Auger electrons in the ion system. The triplet of corresponding angles Ψ_1, Ψ_2 (for incidence), and α (for observation) is then found according to the choice of the line representing the surface ($\Psi_1=20°$ in the experiment).

spectra with the Auger peaks shifted to different energies would not be useful for the present purpose. This is important here because the peak energy shows a strong kinematic shift, different for both ion energies, depending on the observation angles with respect to the beam. There is one single angle α above the surface where the observed peaks have equal laboratory energies for both ion beams.

This special angle of observation can be determined, for any two angles of incidence, by geometrical arguments (see Fig. 1). The set of three angles Ψ_1,Ψ_2, and α will be referred to as *corresponding angles*. For the present conditions, α varies from 86° to 66° when Ψ_2 is varied from 29° to 20°. Two spectra measured at corresponding angles will be termed a pair of *corresponding spectra*. Corresponding spectra will agree as far as the energy of the unperturbed Auger peak is regarded, but they will differ in shape and absolute intensity unless the two ion beams produce (practically) the same depth distribution of Auger emission. It is noted that this criterion will be most sensitive for variations in the depth distribution in the region contributing strongly to the spectrum, i.e., at shallow depth z or early emission time t, where the collisional component of the activity function is still predominant.

The whole procedure was checked by means of numerical simulations with the IOR code [16,21,23]. Using a simple two-exponential form of the activity function, it was confirmed that the corresponding spectra will behave as expected. They are clearly different in shape and intensity when, e.g., the input activity functions $A_V(t)$ for the two ion energies were formed according to the intrinsic hypothesis, but the collisional hypothesis was used to select the incidence angles Ψ_1 and Ψ_2, and vice versa. The simulations have also shown, however, that the corresponding spectra will never be completely identical, not even if Ψ_1 and Ψ_2 were adjusted to give identical depth distributions of emission and the measurements were made at the corresponding angle α. The reason is [16,22,21] that the ion motion affects the peak shape: the faster the ions, the broader the peak and the less its maximum intensity. Fortunately, this deviation is small, and is restricted to the peak region of the spectra, so that it does not affect the inelastic tail at lower energy.

B. Background subtraction

As was stated above, the criterion of equal corresponding spectra supposes that only the contributions originating in the *K* Auger transition are compared. In particular, the background due to kinetic emission must be removed from the raw data. Therefore, the measurements with O^{7+} projectiles were repeated at exactly the same ion energies and the same angles of incidence and observation, but using O^{6+} projectiles instead. The evaluation of such a matching pair of electron energy spectra is based on a system of two linear equations which relate the measured total spectra, called $O^{7+}(E)$ and $O^{6+}(E)$, respectively, to the desired *K* Auger spectrum $S(E)$, and the rest, $B(E)$:

$$\begin{aligned} O^{7+}(E)&=S(E)+B(E),\\ O^{6+}(E)&=\lambda S(E)+B(E). \end{aligned} \tag{1}$$

The component $\lambda\ S(E)$ comes from the fraction of metastable $O^{6+}*$ ions in the O^{6+} beam. λ is of the order of 4–5 %, and differs slightly for different pairs of spectra. This approach involves two important assumptions.

(i) O^{7+} and $O^{6+}*$ projectiles produce identically shaped *K* Auger spectra $S(E)$. This can safely be assumed for the main contribution, i.e., the *KLL* emission which in both projectiles takes place mainly after the *L* shell has been filled up to neutrality. Other minor contributions might be different. However, they will be without importance here, due to their weakness and the smallness of λ.

(ii) O^{6+} and O^{7+} projectiles produce the same background $B(E)$, regarding its absolute intensity and shape. As far as the intensity is considered, this assumption is supported by the findings of Hughes *et al.* [24], who studied the total secondary electron emission for $N^{5+,6+}$ projectiles incident on Au. After allowing for the difference in potential emission they found the total kinetic emission to be dependent on the ion energy but not on the presence or absence of a *K*-shell hole in the incident ions. Recent studies by Aumayr [25], for several projectile target combinations, have shown, however, that there is a slight q dependence of the total yield of kinematic emission which is not yet fully understood [26]. The energy spectrum of kinetic emission from solids induced by highly charged ion bombardment is poorly known for the higher electron energies which are of interest here. The reason lies in the difficulty of separating the continuum from the Auger peaks and their inelastic tails. While it is commonly agreed that $B(E)$ has an approximately exponential shape, even the energy dependence of its slope is still debated [27]. Therefore, we took care to have both the O^{6+} and O^{7+} spectra measured at the same kinetic energy. Furthermore,

the shape of the background $B(E)$ was analyzed in a separate study [28] for the present experimental conditions and in a wide range of observation angles. In this study the validity of the simple system of model equations (1) could also be confirmed. As a result, the desired spectrum $S(E)$ is obtained as the difference spectrum $[O^{7+}(E)-O^{6+}(E)]$ from the measurements, except for a constant factor $1/(1-\lambda)$ which, however, is so close to unity that it can be omitted in practice.

C. Measurements

The measurements were performed at the 14-GHz electron-cyclotron-resonance (ECR) ion source at the Ionenstrahl-Labor (ISL) at the Hahn-Meitner Institut Berlin [29]. Ion beams of O^{7+} or O^{6+} (20–40 nA) at kinetic energies of 51 and 102 keV were focused onto a Cu target mounted in a UHV chamber [30] (base pressure 10^{-8} Pa). The beam width was less than 1.5 mm, as was determined by measuring the current on a thin wire moved across the target position. The ion current was measured from time to time in a separate Faraday cup. The total target current was continuously monitored to control the data acquisition. The target was prepared *in situ* by cycles of sputter cleaning and annealing, and was checked by Auger electron spectroscopy. The crystallinity was proven through Laue diagrams. The electron spectra were taken with an electrostatic parallel plate tandem spectrometer of 5% resolution and 2×10^{-4}-sr acceptance angle.

The glancing angle of incidence for the 102-keV ions was kept constant at $\Psi_1=20°$ throughout the measurements, as a reference condition. For the search for the condition of equal emission depth distributions, the incidence angle Ψ_2 of the 51-keV ions was decreased in steps of 3° from 29° down to 20°, i.e., from the condition valid for the intrinsic hypothesis to that for the collisional hypothesis. For each choice of Ψ_2, the corresponding angle α was determined as described above, and was used to observe four spectra, i.e., for both ion species, O^{7+} and O^{6+}, at both energies each.

The absolute normalization in terms of electrons per incident ion was obtained from the raw spectral data recorded in target current normalization, using the measured ratios of target current to ion current, and correcting for the geometric conditions regarding the sizes of the beam spot and the field viewed by the detector. No dark current or other background has been subtracted. The final K Auger spectra $S(E)$ were then obtained as the difference spectra of O^{7+} and O^{6+}, as was explained above.

III. RESULTS

The four pairs of corresponding spectra of K Auger electrons emerging from the solid are shown in Fig. 2 in absolute normalization. The solid lines are for the 102-keV ions, and the dashed lines for the 51-keV ions. Despite the broad width of the Auger peaks the Doppler shift is noticeable. Within each pair the two peaks agree well in energy. This demonstrates that the KLL transition takes place in both ions from (practically) the same electronic configurations. Comparison to atomic structure calculations made by means of the COWAN codes [31] shows good agreement with the observed energy when the L shell is filled up to neutrality.

We discuss now the absolute peak intensity (the thin horizontal lines in Fig. 2 indicate constant peak *height*). The spectra for 102 keV (solid lines) are all taken with the same incidence angle $\Psi_1=20°$, i.e., from one single depth distribution of emission. From top to bottom in Fig. 2 the observation angle α becomes more distant from the surface normal, and the height of these peaks decreases slightly. This is in agreement with the approximately cosenoidal shape of the angular distribution expected. The series of the Auger peaks for 51-keV ion energy (dotted lines), however, shows opposite behavior. Here the cosenoidal decrease is overcompensated for by a marked increase because of the shallower emission as the angle of incidence varies from 29° to 20°. In the bottom pair of spectra (i.e., for equal angles of incidence) the peak for the 51-keV ions is much stronger than for the 102-keV ions, indicating that the slower moving ions emit at shallower emission depth than the faster ones. This is expected here unless the collisional hypothesis were true for the time evolution of the deexcitation cascade. In the top pair of spectra the order of the peaks is reversed, indicating that the 51-keV ions have deeper-reaching emission sites. It is recalled that here the ions of both energies have equal vertical velocity and reach the same depth at the same time after surface impact. Peaks of equal intensity would be expected in the top pair of spectra if the intrinsic hypothesis were true. However, the most similar peak integrals are seen for $\Psi_2=26°$. This indicates the best agreement of depth distributions for both ion energies. Hence, it can already be inferred from the integrals of the Auger peaks that slower ions need longer times to complete their K Auger transition.

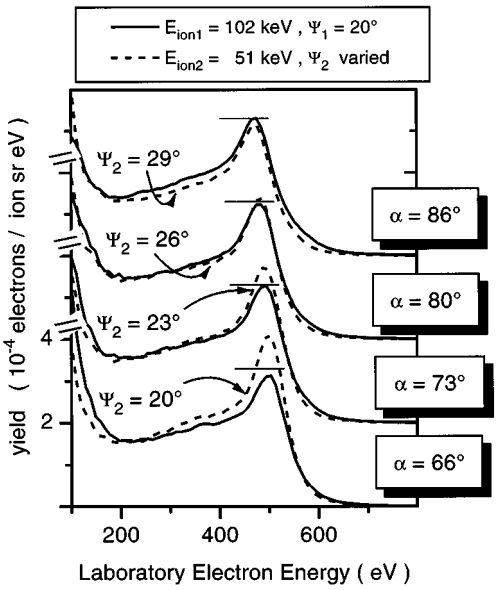

FIG. 2. Four pairs of corresponding K Auger spectra from O^{7+} projectiles in Cu. Solid lines: $E_{ion1}=102$ keV, $\Psi_1=20°$. Dashed lines: $E_{ion2}=51$ keV, $\Psi_2=29°$, 26°, 23°, and 20° (from top to bottom). The top pair of spectra represents the case of equal vertical velocity of the ions at both energies. The best agreement of shape and intensity is seen for $\Psi_2=26°$, i.e., where the 51-keV ions move at slower vertical velocity than the 102-keV ions. This demonstrates that the slower moving ions need longer times to deexcite by K Auger transition.

This evaluation can be made more sensitive if the information contents of the whole energy spectra is used instead

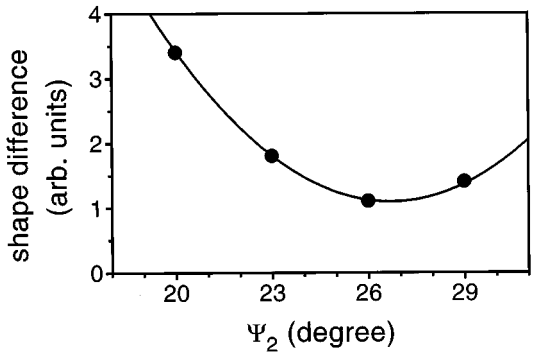

FIG. 3. The measure of difference of shape for the four pairs of corresponding spectra shown in Fig. 2. The line is to guide the eye. The best agreement is obtained about $\Psi_2 = 26 \ldots 27°$.

of the absolute peak height alone. Moreover, the absolute intensity can never be determined experimentally with the same degree of precision as the spectral shape. We therefore repeat the analysis of the corresponding spectra of Fig. 2, but concentrate now on the spectral shapes. Visual inspection shows already that the same pair of spectra identified above as having almost equal peak intensities also show the most similar shapes of their peaks and inelastic tails (down to the lowest electron energies). The remaining difference in peak shape will be discussed below.

In order to show that this identification of best matching shapes does not depend on the absolute normalization of the spectra shown, the comparison of shapes was repeated by means of a numerical fit. One of the spectra of each pair was fitted to the other by multiplication with a constant factor, and then was subtracted from it to form the difference spectrum. The integral of the squared difference spectrum indicates the goodness of the best fit. This is shown in Fig. 3 for each of the four pairs of corresponding spectra. The minimum shape deviation is observed again for $\Psi_2 = 26°$. (We note that the smooth curve drawn through the points could indicate that an even better agreement would be obtained at 27°, but still significantly below the intrinsic limit, 29°.)

IV. DISCUSSION

A. Velocity-dependent side feeding

The set of corresponding spectra demonstrates in the first place that the depth distributions of the *K* Auger emission from ions of different energy but equal vertical velocity (see top pair of spectra in Fig. 2) are different. The deviation observed confirms the expected picture that in this case the slower-moving ions emit at greater depth because they need a longer time for their deexcitation. In the experiment this deviation was compensated for by directing the slower ions toward the solid with smaller vertical velocity. The effect observed is clear but not very strong. Before it can be attributed to the velocity-dependent side feeding, we exclude several potentially interfering processes.

First, we consider the possible consequences of the experimental uncertainty of the absolute spectral intensity. It is noted that our evaluation is not completely independent of any normalization of the spectra, because the complete cancellation of the common background $B(E)$ is assumed when the difference spectrum $O^{7+}(E) - O^{6+}(E)$ is formed [see Eqs. (1)]. The uncertainty in the absolute normalization might amount to up to 10%. However, in view of the approximately exponential decrease of $B(E)$, an incomplete background cancellation would bear very little influence on the *K* Auger spectra $S(E)$ except for the lowest electron energies, where an incomplete cancellation would cause a strong increase (or decrease). Such an increase can be seen, indeed, in all Auger spectra $S(E)$ of Fig. 2. Exactly this behavior, however, is expected from the collision cascade of secondary electrons generated by the primary Auger electron itself. If the collision cascade is included in the electron transport model IOR [23], the simulated spectra show good agreement with the increase observed towards lower electron energy. Moreover, it is seen in Fig. 2 that again the case $\Psi_2 = 26°$ shows the best agreement in this low-energy region. Therefore it can be excluded that the agreement observed at 26° would be the result of a normalization error.

Another potentially disturbing effect is the scattering of the ions which, however, is negligible here, and could gain importance only in experiments with lower ion energies. In this case, the observable consequence would be that the slower ions are scattered slightly more strongly, and therefore do not penetrate as easily as the faster ions do. In order to obtain a pair of equal corresponding spectra, the slower ions must be directed more steeply into the solid to reach the same average depth after the same time, opposite to the present findings at energies high enough to ensure straight-line trajectories.

However, even in the best matching case of $\Psi_2 = 26°$ the two corresponding spectra do not agree completely. The Auger peak of the slower ions has practically the same integral as for the faster ones, but is slightly narrower and higher. This could suggest that an angle Ψ_2 slightly greater than 26° would give an even better matching of the spectra. In our opinion, however, this shape difference is exactly the aforementioned velocity effect which was predicted from simulations with the IOR code [22,21], and that it is observed here for the first time, to our knowledge. The expected and observed modification of the shape is readily explained as a type of Doppler broadening induced by the electron-solid interaction. The Auger peak in the spectrum, observed in a certain direction of detection, is mainly formed by electrons, which on their way out of the solid suffered a few elastic deflections only, most of them in the forward direction within the cone of the forward maximum of elastic electron-atom scattering. Hence the initial directions of these electrons are spread over a certain range of angles. Due to the kinematic energy shift, this range of angles corresponds to a certain spreading of the electron energies. The width of this energy spread grows with the ion velocity, and the maximum peak height is reduced accordingly. This scenario agrees well with the corresponding spectra shown in Fig. 2. (We note that this effect has been ignored in the numerical comparison of the shapes, shown in Fig. 3. If it could have been included, the minimum of the curve drawn through the points would be shifted to smaller Ψ_2, i.e., closer to 26° and further away from 29° where the normal velocities are equal.)

Therefore we are led to the result that $\Psi_2 = 26°$ is the angle of incidence where O^{7+} ions of 51 keV have their depth distribution of *K* Auger transitions most similar to that

of 102-keV ions at $\Psi_1 = 20°$. At these angles, the normal velocity of the 102-keV ions is 1.1 ($=\sin 29°/\sin 26°$) times faster than that of the 51-keV ions. We conclude that the K Auger emission of 102-keV ions develops 1.1 times faster than that of 51-keV ions. This value for the velocity dependence of the K Auger deexcitation is derived in a way practically independent of any model assumption besides that of straight-line motion of the ions.

B. Comparison to cascade models for the deexcitation

In models of the deexcitation of highly charged ions moving inside a solid, the conduction band is a source of any number of electrons required. Since for highly charged ions of first-row elements only the L and K shells fall clearly below the conduction band, the electron cloud neutralizing the ion can be approximated when its M shell is appropriately populated [32]. This situation is remarkably simpler than for the above-surface-deexcitation cascade [1,9,33] which involves much more electronic shells.

In a simple cascade model, the ion is supposed to enter the solid with its L shell still empty. Only two steps are then considered: the filling of the L shell up to some average occupation number, and the Auger transition to fill the K shell. The activity function depends on the time constants for each of the steps, and has the form (if properly normalized)

$$A(t) = \frac{e^{-t/\tau_L} - e^{-t/\tau_K}}{\tau_L - \tau_K}. \tag{2}$$

This model was introduced in Refs. [4,5] for N^{6+} ions moving in Cu and Au targets with 60 keV ($V_{\text{ion}} = 0.4$ a.u.). For τ_K, these authors took the free-atom value for neutral N ($\tau_K = 400$ a.u.), and found, as the best-fit values, $\tau_L = 80$ a.u. for the Cu target and $\tau_L = 400$ a.u. for Au. The two-step model was also used in [10,11] to analyze experiments with Ne^{9+} ions on Al targets at somewhat lower ion velocities between $V_{\text{ion}} = 0.017$ and 0.21 a.u. These authors also used a constant value $\tau_K = 66$ a.u., and found τ_L to vary in inverse proportional to the ion velocity (except for the slowest one), roughly as

$$\tau_L = 5/V_{\text{ion}} \quad \text{in a.u.} \tag{3}$$

This dependence on V_{ion} is typical for a process entirely controlled by collisions, and with a velocity-independent cross section. The cross section which can be estimated from this equation is 16 a.u. per lattice atom, i.e. about the geometric size of the primitive lattice cell. When Eq. (3) is used for the same ion velocity as in Refs. [4,5] the result is $\tau_L = 12$ a.u. only. The spread in τ_L values for ions of the same velocity may partly be ascribed to the different ion-target combinations, but also may be regarded as a hint about the approximative character of the models used to evaluate the experiments.

No study of the deexcitation cascade of O^{7+} ions has been done so far, to our knowledge. Since the velocity dependence of the deexcitation process has been demonstrated in the present experiment, we will use here the velocity-dependent τ_L of Eq. (3). This gives $\tau_L = 10$ and 14 a.u. for the O ions of 102 and 51 keV, respectively. The parameter τ_K in Eq. (2) is for the lifetime of the ''typical'' intermediate level. Considering the probably completely filled L shell, we take the free-atom KLL lifetime which is estimated as $\tau_K = 200$ a.u. [20]. This step of the deexcitation is of intrinsic character.

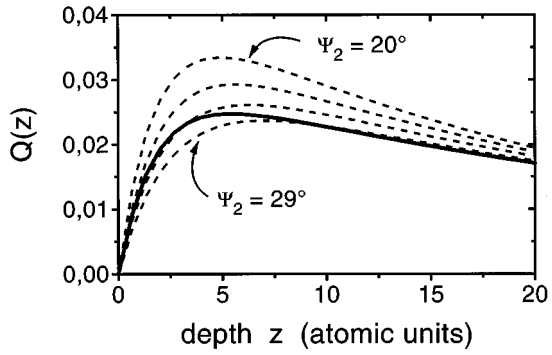

FIG. 4. The depth distributions of K Auger emission, according to the two-step model. Solid line: $E_{\text{ion1}} = 102$ keV and $\Psi_1 = 20°$; dashed lines: $E_{\text{ion2}} = 51$ keV and $\Psi_2 = 29°$, 26°, 23°, and 20° (from bottom to top).

Figure 4 shows the depth distributions of K Auger emission, as calculated with the activity function from Eq. (3). The figure covers the shallow subsurface region most important for the present experiment. The solid line is the reference depth distribution of 102-keV ions at $\Psi_1 = 20°$, and the four dashed lines are for the trial angles for 51-keV ions, $\Psi_2 = 29°$, 26°, 23°, and 20° (from bottom to top). The curve with smallest maximum intensity corresponds to the steepest incidence, $\Psi_2 = 29°$, where the ions spend the shortest time in the region near the surface. The density of emission is seen to increase when Ψ_2 is reduced. This corresponds well to the systematic increase of peak height in the Auger spectra for 51 keV (from top to bottom in Fig. 2). With respect to the reference curve for 102 keV, the best matching depth distribution of the 51-keV ions is obtained at $\Psi_2 = 26°$, i.e., in agreement with the experimental result. It is noted, however, that there is no way to make these model depth distributions exactly identical for different ion velocities. Nevertheless, there is good agreement between the picture emerging from the simple two-step model and the experimental results presented above, taking the approximative character of the model and the practical limits of uncertainty in the spectrum normalization into account.

It is interesting to note that the agreement cannot be improved by choosing increased τ_L values, like those quoted above. On the contrary, this would strengthen the collisional component of the process. The depth profiles of the 51-keV ions would change relative to the 102-keV reference distribution, and we would find the best matching one for a Ψ_2 closer to the value for the purely collisional case, i.e., closer to 20°.

Moreover, the agreement is likely to deteriorate in the same sense if the model is refined by introducing recent information available from the advanced multistep cascade models for Ne^{9+} ions in Al [13,14], and N^{6+} ions in Si and Au [12] (valid, however, at lower ion energies). In first place, the cross section for the collisional electron transfer should be reduced, according to calculations based on molecular-orbital schemes which include the interaction of the ion with the electron gas [14,32]. The estimates for the cross sections

are of the order of 10 a.u. (on the average) for each one of the individual electron transfer steps to the L shell. This gives a much longer filling time τ_L than adopted above, and would lead to a strong enhancement of the collisional component of the cascade. In consequence, the best matching depth distribution would be predicted for an angle closer to the value for the collisional cascade, $\Psi_2 = 20°$. Furthermore, if the filling cross sections were considered to increase with the ion energy, the velocity dependence of τ_L would be even stronger, which again would reduce the weight of the intrinsic processes in the cascade.

There is one effect more which also leads to an increase of the collisional component. In the multistep models the sequential transfer of electrons to the L shell is treated explicitly, and the K Auger transition may occur in the ion with any L-shell occupation greater than 1. Although the K Auger transition from a sparsely populated L shell is considerably slower than in the neutral atom [20,13,14], part of the observed K Auger peak is emitted from the early stages of the cascade. Therefore, the effective K Auger lifetime, which was taken to be constant in the simple models, becomes dependent on the average L-shell population during the cascade. It becomes shorter at increased ion velocity because then the L-shell filling is accelerated. On the one hand, this makes the two activity functions look more like bell curves (e.g., Ref. [13], Fig. 6) which differ only by a certain stretching factor. This would suggest that in principle a much better matching of the depth distributions than that of Fig. 4 can be obtained by the present experimental technique. On the other hand, the same effect again adds to the collisional component of the deexcitation process. Consequently, if the models of Refs. [13,14] are roughly adapted to the present experiment, preliminary calculations show that they predict a wrong incidence angle Ψ_2 close to 23° for the optimum matching of the depth distributions.

The reason for this discrepancy is not yet clear. Recent theoretical work [34] seems to indicate that direct electron transfer from the conduction band to the closely lower-lying projectile L shell would apport considerably to the intrinsic part of the deexcitation cascade because (i) it depends only weakly on the velocity; and (ii) it is extremely fast in the present case of ions where the L-shell energy lies very close below the conduction band, so that only little energy must be transferred to the electron gas. These calculations give L-shell filling rates one order of magnitude faster than the values used in Refs. [13,14]. With these electron transfer rates the best matching pair of model depth distributions would likely be found at the same angle $\Psi_2 = 26°$, as measured.

V. CONCLUSIONS

The influence of the velocity on the deexcitation of hydrogenlike O^{7+} ions incident on a Cu(111) surface was studied by means of secondary electron spectroscopy. The projectile energies are such that the emitting ions move with constant velocity along straight-line trajectories within the solid. The depth profile of K Auger emission was evaluated considering that the electron energy spectra reflect the amount of interactions of the emitted electrons with the solid on their way out to the surface. The uncertainties associated with the use of quantitative electron transport models were avoided by means of the method of corresponding spectra. This interesting method essentially consists in a difference measurement of spectral shape. Irradiation and observation conditions of the corresponding spectra are designed such that, ideally, the observation of two spectra which have equal shapes indicates that their emission depth profiles must be equal too. Using this method it was shown that the deexcitation cascade of O^{7+} ions in copper develops 10% faster at 102 keV than at 51-keV ion energy. This acceleration, observed here in a way quite independent of any specific model for the ion and electron transport, confirms and extends the results known from measurements of Ne^{9+} in aluminum in the regime of lower velocities.

Unfortunately, the method of corresponding angles cannot be applied straightforwardly to this interesting regime where the velocity effect on the deexcitation cascade is much stronger, because part of the model independence achieved in the present experiment will be lost when at lower ion energy the scattering of the trajectories must be taken into account.

Furthermore, the two corresponding spectra obtained with different ion energies but equal depth distribution of emission made possible to prove a combination effect of the ion velocity and the electron scattering on the peak shape. This shape modification has been predicted from Monte Carlo simulations of the electron spectra as an analog to the Doppler broadening known from isotropically moving sources, and it is seen here for the first time in this experiment, to our knowledge.

The method of corresponding spectra seems well suited to provide data on the influence of the ion velocity on the neutralization-deexcitation processes of highly charged ions in solids. These data can be useful in an evaluation of advanced multistep cascade models.

ACKNOWLEDGMENTS

We gratefully acknowledge the cooperation of W. Heiland and his group (U. Osnabrück) in making the Laue diagrams of the target, and of H. Waldmann for his assistance with the measurements. The present authors, who are from the University of Bremen, also express their deep thanks to N. Stolterfoht for giving us the opportunity to make these experiments and helping us with innumerable discussions. Financial support from Stiftungsverband Regenbogen for one of us (A. S.) is gratefully acknowledged.

[1] H. J. Andrä, Nucl. Instrum. Methods Phys. Res. Sect. B **43**, 306 (1989).

[2] L. Folkerts and R. Morgenstern, Europhys. Lett. **13**, 377 (1990).

[3] J. P. Briand, L. de Billy, P. Charles, S. Essabaa, P. Briand, R. Geller, J. P. Desclaux, S. Bliman, and C. Ristori, Phys. Rev. Lett. **65**, 159 (1991).

[4] F. W. Meyer, S. H. Overbury, C. C. Havener, P. A. Zeijlmans

van Emmichoven, and D. M. Zehner, Phys. Rev. Lett. **67**, 723(1991).
[5] F. W. Meyer, S. H. Overbury, C. C. Havener, P. A. Zeijlmans van Emmichoven, J. Burgdörfer, and D. M. Zehner, Phys. Rev. A **44**, 7214 (1991).
[6] J. Das, L. Folkerts, and R. Morgenstern, Phys. Rev. A **45**, 4669 (1992).
[7] J. Das and R. Morgenstern, Phys. Rev. A **47**, R755 (1993).
[8] H. J. Andrä, A. Simionovici, T. Lamy, A. Brenac, G. Lamboley, J. J. Bonnet, A. Fleury, M. Bonnefoy, M. Chassevent, S. Andriamonje, and A. Pesnelle, Z. Phys. D **21**, 135 (1991); H. J. Andrä, A. Simionovici, T. Lamy, A. Brenac, and A. Pesnelle, Europhys. Lett. **23**, 361 (1993).
[9] J. Burgdörfer, in *Fundamental Progress and Applications of Atoms and Ions*, edited by C. D. Lin (World Scientific, Singapore, 1993), p. 517.
[10] R. Köhrbrück, M. Grether, A. Spieler, N. Stolterfoht, R. Page, A. Saal, and J. Bleck-Neuhaus Phys. Rev. A **50**, 1429 (1994).
[11] M. Grether, A. Spieler, R. Köhrbrück, and N. Stolterfoht, Phys. Rev. A **52**, 426 (1995).
[12] J. Limburg, S. Schippers, I. Highes, R. Hoekstra, and R. Morgenstern, Phys. Rev. A **51**, 3873 (1995).
[13] R. Page, A. Saal, J. Thomaschewski, L. Aberle, J. Bleck-Neuhaus, R. Köhrbrück, M. Grether, and N. Stolterfoht, Phys. Rev. A **52**, 1344 (1995).
[14] N. Stolterfoht, A. Arnau, M. Grether, R. Köhrbrück, A. Spieler, R. Page, A. Saal, J. Thomaschewski, and J. Bleck-Neuhaus, Phys. Rev. A **52**, 445 (1995).
[15] S. Schippers, J. Limburg, J. Das, R. Hoekstra, and R. Morgenstern, Phys. Rev. A **50**, 540 (1994).
[16] J. Bleck-Neuhaus, R. Page, and A. Saal, Radiat. Eff. Defects Solids **130-131**, 157 (1994).
[17] S. Schippers, S. Hustedt, W. Heiland, R. Köhrbrück, J. Bleck-Neuhaus, J. Kemmler, D. Lecler, and N. Stolterfoht, Phys. Rev. A **46**, 4003 (1992).
[18] S. Hustedt, N. Hatke, W. Heiland, J. Limburg, I. G. Hughes, R. Hoekstra, and R. Morgenstern, Nucl. Instrum. Methods Phys. Res. Sect. B **98**, 454 (1995).
[19] M. T. Robinson, Phys. Rev. B **40**, 10 717 (1989).
[20] N. Vaeck and J. E. Hansen, J. Phys. B **28**, 3523 (1995).
[21] J. Bleck-Neuhaus, A. Saal, R. Page, and P. Biermann, Phys. Rev. A **49**, R1539 (1994).
[22] J. Bleck-Neuhaus, R. Page, and A. Saal, Nucl. Instrum. Methods Phys. Res. Sect. B **78**, 113 (1993).
[23] A. Saal, Ph.D. thesis, University of Bremen, 1995.
[24] I. Hughes, J. Burgdörfer, L. Folkerts, C. C. Havener, S. H. Overbury, M. T. Robinson, D. M. Zehner, P. A. Zeijlmans van Emmichoven, and F. W. Meyer, Phys. Rev. Lett. **71**, 291 (1993).
[25] F. Aumayr (private communication).
[26] A. Arnau (private communication).
[27] P. Zeijlmans van Emmichoven, C. Havener, I. Hughes, D. Zehner, and F. Meyer, Phys. Rev. A **47**, 3998 (1993).
[28] L. Aberle, A. Saal, R. Page, J. Thomaschewski, J. Bleck-Neuhaus, M. Grether, A. Spieler, and N. Stolterfoht (unpublished); L. Aberle, Master's thesis, University of Bremen, 1995.
[29] B. Martin, M. Grether, R. Köhrbrück, U. Stettner, and H. Waldmann, Kernfysisch Versneller Instituut Report No. 996, 1993 (unpublished), p. 188.
[30] See. Ref. [17].
[31] R. D. Cowan, *The Theory of Atomic Structure and Spectra* (California Univeristy Press, Berkeley, 1981); S. Schippers, KVI Internal Report No. KVI-189i, 1994 (unpublished).
[32] A. Arnau, R. Köhrbrück, M. Grether, A. Spieler, and N. Stolterfoht, Phys. Rev. A **51**, R3399 (1995).
[33] J. Burgdörfer, P. Lerner, and F. W. Meyer, Phys. Rev. A **44**, 5674 (1991).
[34] R. Diez Muino, N. Stolterfoht, A. Arnau, A. Salin, and P. M. Echenique, Phys. Rev. Lett. **76**, 4639 (1996); R. Diez Muino, A. Arnau, and P. Echenique, Nucl. Instrum. Methods Phys. Res. Sect. B **98**, 420 (1995).